American Ecological Engineering Society

Journal of Ecological Engineering Design
journals.uvm.edu/jeed

Research Paper

Assessing Environmental Drivers of Denitrification in Restored Riverine Floodplains

Danielle Winter Lay[1], Sara W. McMillan[2], Jacob D. Hosen[3], Sayan Dey[4], Gregory B. Noe[5]

[1]Purdue Extension, Purdue University, West Lafayette, Indiana, United States

[2]Agricultural and Biosystems Engineering, Iowa State University, Ames, Iowa, United States

[3]Forestry and Natural Resources, Purdue University, West Lafayette, Indiana, United States

[4]Taylor Geospatial Institute, Saint Louis University, St. Louis, Missouri, United States

[5]U.S. Geological Survey, Florence Bascom Geoscience Center, Reston, Virginia, United States

Correspondence
Danielle Winter Lay
Purdue Extension
Purdue University
West Lafayette, IN 47907, USA

Email: winter35@purdue.edu

Received
September 26, 2024

Accepted
April 20, 2025

Published
March 5, 2026

Editors
Mauricio E. Arias, Editor in Chief

Eric D. Roy, Associate Editor

Restoration of impaired floodplains is an increasingly prevalent strategy for alleviating water quality concerns and reducing downstream flooding at watershed scales. Floodplains temporarily store water and slow flow velocity to promote sedimentation during overbank flooding and remove inorganic nitrogen from floodwater and groundwater via denitrification. Evaluating the impacts of different restoration strategies on denitrification can inform more strategic investments into floodplain modifications that improve water quality outcomes. Our research investigates how denitrification rates in floodplains respond to environmental factors that are actionable from an engineering perspective through design and water resources management. We seasonally measured soil denitrification enzyme activity and various environmental characteristics in 4 floodplains with different restoration design and management approaches at the confluence of the Wabash and Tippecanoe Rivers in Indiana, United States. Our results showed that denitrification rates in an agricultural floodplain were significantly lower than in restored floodplains with native vegetation. Certain soil conditions characteristic of floodplain wetlands were associated with higher denitrification, particularly elevated total nitrogen, moisture, silt, and organic matter contents. Vegetation species composition was correlated with denitrification rates. This link may reflect the direct effects of vegetation on soil conditions, such as supplying labile organic carbon, or indirect effects, such as vegetation acting as an indicator of hydrologic regime and land use. Denitrification seasonally varied, peaking in winter when nitrate supply from rivers draining agricultural watersheds in the region is also high. Substrate limitation of soil denitrification enzyme activity was most significant during the summer when overbank flooding, which replenishes soil nitrogen stocks, rarely occurs. Our findings indicate that denitrification capacity will likely be maximized in riverine floodplains that are restored as wetlands with diverse native vegetation and enhanced hydrologic connectivity. Such restoration activities promote higher denitrification rates via elevated moisture, fine sediment deposition, and soil organic matter.

Keywords Denitrification, Floodplain Restoration, Agricultural Floodplains, Floodplain Vegetation

Lay DW, McMillan SW, Hosen JD, Dey S, Noe GB. 2026. Assessing environmental drivers of denitrification in restored riverine floodplains. J Ecol Eng Des. https://doi.org/10.70793/jeed.13

1. Introduction

Floodplains mediate fluxes of sediment and nutrients, especially nitrogen (N), between terrestrial, atmospheric, and aquatic environments (Junk et al. 1989; Naiman and Decamps 1997; Tockner et al. 1999). Floodplains store floodwater, act as a sink for sediment and sediment-associated nutrients and carbon (C), and retain and transform excess N. Floodplains temporarily retain high levels of riverine N, which can be subsequently transformed and permanently removed from the system via denitrification (Noe and Hupp 2009; Roley et al. 2012; Clilverd et al. 2016; Natho et al. 2020; Noe et al. 2022; Quine et al. 2022). However, most floodplains in the Mississippi River Basin (MRB), United States, have been converted from forests, wetlands, and prairies to agricultural and developed areas (Rajib et al. 2021; Tockner and Stanford 2002). Further, widespread levee installation, reservoir management, main channel downcutting, and accumulation of legacy sediment have diminished the frequency and duration of surface water connections via overbank flooding (Noe and Hupp 2005; Theiling and Nestler 2010; Heine and Pinter 2012; Federman et al. 2023). Artificial drainage to support agricultural production lowers water table elevations, limiting subsurface connections (Jaynes and Isenhart 2014). This decreased hydrologic connectivity, defined as the frequency, magnitude, and duration of overbank flooding and shallow groundwater flow that supports exchanges of water and materials between rivers and floodplains, results in more N being transported downstream rather than stored and processed in floodplains (Harvey et al. 2018). Decreased retention of N in floodplains has coincided with increasing inputs of biologically available N to waterways from intensive agriculture and development (Galloway et al. 2004; Tian et al. 2020). Advancements have been made in developing and implementing conservation practices (e.g., woodchip bioreactors, two-stage ditches, cover crops) that reduce N export from farming operations. However, excess N loads are still reaching waterways (García et al. 2016).

Restoration and creation of non-floodplain wetlands is a key strategy for combating excess N delivery to waterways within the MRB. Yet, even if all 8,000 km^2 potential restorable non-floodplain wetlands in the Upper MRB are rehabilitated, these restoration efforts would only reduce annual loads of nitrate (NO_3^-) by 12%, falling short of the target reductions needed to reduce hypoxia in the Gulf to less than 5,000 km^2 (Evenson et al. 2021). Thus, improved strategies for designing and managing restorations and other ecological engineering practices to support higher NO_3^- removal rates can help address this deficit. N removal in floodplains is influenced by denitrification capacity, incoming NO_3^- supply, and residence time (Harvey et al. 2018; Welti et al. 2012). Floodplains can be restored and managed to optimize these factors (e.g., Forshay and Stanley 2005; Sheibley et al. 2006). Because of their position in the landscape, highly functioning floodplains can remove excess N that has not been captured by in-field and edge-of-field conservation practices, so floodplain restoration in the MRB can be a complementary strategy for meeting N loading reduction targets.

Denitrification, or the stepwise microbial process that reduces NO_3^- to gaseous N_2, is often the dominant pathway for NO_3^- removal in floodplains and represents a permanent sink for NO_3^- (Olde Venterink et al. 2006; Lutz et al. 2020; Li and Twilley 2021). Thus, floodplain restoration and conservation projects can increase NO_3^- removal rates by promoting the formation of environmental conditions that are optimal for denitrification and ensuring that as much excess NO_3^- is delivered to these restoration sites as possible. Requisite soil conditions for denitrifiers to remove excess NO_3^- are well-understood: a supply of labile organic matter or other reduced compounds and anoxic conditions (Reddy and DeLaune 2008). However, how ecological engineers can design floodplain restoration practices that maximize these desirable soil environmental conditions is less clear. Assessing how plot-, field-, and catchment-scale characteristics that are more directly manipulated by design and management relate to denitrification can help to generate actionable strategies from an ecological engineering perspective to increase NO_3^- removal via denitrification. For example, catchment-scale characteristics, such as the percentage of forest and urban cover, have been identified as predictors of denitrification in floodplains (Korol et al. 2019). Spatially targeted wetland restoration shows potential to reduce N loading even further, with optimized scenarios reducing N loading from the MRB by more than 50% (Cheng et al. 2020). Such insights can guide practitioners in selecting sites to maximize the effectiveness of floodplain restoration and modification projects for a given financial investment.

Passive restoration strategies focus on minimizing or eliminating disturbances, such as agricultural land retirement or grazing exclusion. Active restoration strategies aim to accelerate the rate of ecosystem recovery after the disturbance is addressed through additional design and management actions. Active restoration approaches span a continuum of effort and investment, with more expensive, intensive interventions typically resetting ecosystems closer to pre-disturbance conditions (Atkinson and Bonser 2020; Jones et al. 2018). More active restoration approaches that reset floodplain geomorphological

Highlight

Denitrification rates and potential in riverine floodplains vary with restoration design approach and are predicted by soil and vegetation properties.

structure and, consequently, hydrologic connectivity closer to that of minimally disturbed floodplains, such as levee setbacks and legacy sediment removal, might be the most advantageous interventions for co-benefits to ecosystem function by boosting flood reduction, habitat creation, water quality enhancement, and climate resilience, but these designs require the highest financial investment due to earthwork and related construction costs and compensation for lost agricultural productivity (Opperman et al. 2009; Guida et al. 2016). Lower cost floodplain restoration approaches, such as replanting native vegetation without altering floodplain structure to restore pre-disturbance hydrology, are also used. Yet, the difference in N is removal remains unclear (Orr et al. 2007; Salk et al. 2018).

Direct comparisons of the impacts of restoration strategies along a gradient of intervention under similar prior conditions can be used to determine if and how denitrification capacity scales. These evaluations can be complemented by examinations of the relationships between denitrification rates and restoration characteristics to distinguish which attributes of efficacious restoration strategies likely drive increases in denitrification. Using plot- and field-scale measurements, we aimed to 1) assess patterns of denitrification in floodplains in response to different restoration approaches and 2) identify environmental controls of denitrification that can be incorporated into future restoration design and management strategies. We hypothesized hydrogeomorphic characteristics, such as proximity to drainage and extent of surface connection, would drive variability in denitrification potential, making geomorphic setting and hydrologic connectivity critical design considerations to support more effective floodplain restorations. Identifying actionable controls of denitrification can inform more optimal design and management of restored floodplains for maximum denitrification, thereby reducing N export downstream and protecting water resources.

2. Materials and Methods

2.1. Site Descriptions

We sampled 4 floodplains: a site with row crop agriculture along the Wabash River (WR-A), former agriculture sites along the Wabash River (WR-P) and Tippecanoe River (TR-P) that were restored as prairies, and a mitigation wetland restoration project at a former agriculture site along the Wabash River (WR-W) (Figure 1; Supplementary Figure S1). The 2 prairie sites, WR-P and TR-P, underwent minimal geomorphic modification whereas the wetland site, WR-W, was modified to restore wetland hydrology, representing greater effort and investment along the continuum of active restoration approaches. These model ecosystems are in Prophetstown State Park in Battleground, Indiana, United States, near the confluence of the Wabash River (HUC 051201) and the Tippecanoe River (HUC 05120106). Within each site, we sampled 9 locations that spanned 3 transects, which ran roughly perpendicular to the main channel, to capture variability in geomorphology, hydrology, and vegetation. WR-W is at the confluence of the Wabash and Tippecanoe Rivers and was restored as a complex of wetlands and channels in 2008 and 2010 for mitigation credit after being retired from crop production in 2004 along with TR-P and WR-P. This more intensive restoration project involved removing artificial drainage infrastructure, stabilizing riverbanks, creating trails and accessways, and restoring bottomland forests, ephemeral channels, tall grass prairies, emergent marshes, and sedge meadows. Unlike other sites, WR-W receives floodwater from both rivers first through ephemeral channels and then overbank flooding. Dominant plant communities in WR-W during the period of sampling included monocultural patches of reed canary grass (*Phalaris arundinacea*), giant ragweed (*Ambrosia trifida*), big bluestem (*Andropogon geradii*), and Indiangrass (*Sorghastrum nutans*) and highly diverse patches of native shrubs and clumped grasses.

WR-P and TR-P represent less active restoration approaches that do not reset floodplains as closely to pre-disturbance geomorphic structures and hydrology. At these sites, native prairie vegetation was planted, but hydrologic connectivity was not modified through extensive earthwork. TR-P was restored as a prairie and is maintained by periodic burning. TR-P is located upstream of the confluence on the Tippecanoe River and is flooded by the Tippecanoe River. Common plant species in TR-P during the project period were reed canary grass, tall goldenrod *(Solidago gigantea)*, and Indiangrass. WR-P was also restored to native prairie but was maintained with occasional mowing during the project period. WR-P is flooded by overbank flows from the Wabash River and receives hillslope seepage throughout the year. Common plant species in WR-P during the project period included reed canary grass, tall goldenrod, and cutleaf coneflower *(Rudbeckia laciniata)*.

WR-A is used for row crop agriculture and is roughly 1.5 km downstream of WR-P along the Wabash River. Corn was grown during the 2018 and 2020 growing seasons, while soybeans were grown during the 2019 growing season. Fields were tilled after harvest in the fall, cover crops were not planted outside the growing season during the project period, and mineral fertilizers were applied at recommended rates. Floodwaters from the Wabash River primarily enter WR-A through an ephemeral channel.

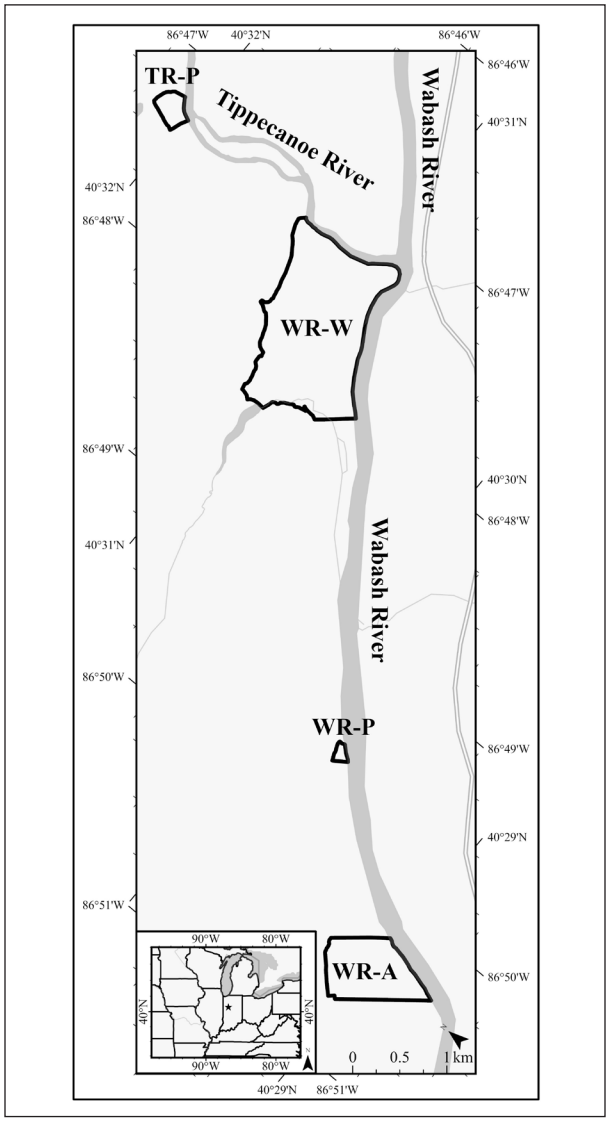

Fig. 1. The locator map indicates where each floodplain site is located with respect to the Tippecanoe and Wabash Rivers. The Tippecanoe River flows from TR-P (study site area: 0.05 km^2) toward WR-W (0.02 km^2). The Wabash River flows from the confluence with the Tippecanoe River near WR-W (1.13 km^2) toward WR-A (0.32 km^2). The inset map shows the location of these sites within the region.

2.2. Assessing Denitrification Potential

We measured denitrifying enzyme activity (DEA) each spring (Mar–May), summer (Jun–Aug), fall (Sept–Nov), and winter (Dec–Feb) from summer 2018 to spring 2020 in floodplain soils via the redox-optimized acetylene (C_2H_2) block method (Tiedje et al. 1989; Groffman et al. 1999). We collected soils with a 2-cm diameter, stainless-steel soil probe from 0 cm – 10 cm depth. Each site included 9 sampling locations (n=9) that were sampled once during each season. We measured DEA in slurries with river water (DEA_{River}) and C- and N-amended water (DEA_{CN}) (47.2 mg $C_6H_{12}O_6$ /L and 60.7 mg $NaNO_3$/L) to represent ambient and optimized concentrations of NO_3^- and labile organic C, respectively. River water samples were collected at each site from the adjacent channel. The water chemistry of added river water is further described in Supplementary Table S2. During summer 2018, we only measured DEA_{River} and added DEA_{CN} for subsequent seasons. To prevent de novo synthesis of denitrification enzymes, we adjusted slurries to a final concentration of 0.21 mM chloramphenicol (Bernot et al. 2003). We collected headspace samples from slurries hourly for 5 hours. Nitrous oxide (N_2O) concentrations were measured with a Shimadzu Gas Chromatograph (GC) (GC-2014, Shimadzu Corporation, Kyoto, JP). We used the Ideal Gas Law and Henry's Law to estimate the combined mass of N_2O in the slurry and headspace and then estimated DEA_{CN} and DEA_{River} rates as the slope of a linear model of mass of N_2O as N (N_2O-N) across time. We then normalized our DEA_{CN} and DEA_{River} rates by oven-dried soil mass of each slurry.

2.3. Concurrently Characterizing Potential Drivers of Denitrification

2.3.1. Soil Properties

We measured soil moisture content gravimetrically (Jarrell et al. 1999). We then measured soil organic matter (OM) content and calcium carbonate ($CaCO_3$) content gravimetrically in dried soils via loss on ignition in series at 550 °C for 5 hours and 950 °C for 1 hour, respectively (Heiri et al. 2001). Air-dried, roughly ground samples were analyzed for total C and N content by combustion on a LECO 628 Series elemental analyzer (LECO Corporation, St. Joseph, Michigan, US). We estimated particle size distribution (10th, 50th, and 90th percentiles) and percent sand, silt, and clay based on the USDA textural soil classification system with air-dried samples that were suspended in a 2.5% sodium hexametaphosphate ($[NaPO_3]_6$) solution on a Mastersizer 3000 via laser diffraction (Malvern Panalytical Ltd, Malvern, UK). We measured bulk density with core sampling (7.5 cm diameter, 10 cm depth) during spring 2018 and

summer 2018 and used the means of these 2 campaigns to represent bulk density for the project period.

2.3.2. Hydrogeomorphic Variables

We represented hydrologic connectivity with numerous metrics: height above nearest drainage area (HAND), horizontal distance to the nearest drainage (HDND), slope to the nearest drainage, and cumulative days flooded for various time periods before sampling. We estimated HAND, HDND, and slope to the nearest drainage (i.e., slope = HAND/HDND) from 1.5-m resolution, LiDAR-based digital elevation models (DEM) from the Indiana Spatial Data Portal using the TauDEM toolbox in ArcMap (Esri, Redlands, California, United States) (Tarboton, 2015). We also classified each sampling location based on the overriding geomorphic influence. If a location did not represent a distinct geomorphic feature, we labeled the location as *floodplain*. Other classifications included *toe-slope*, *backwater*, *ephemeral channel*, and *natural levee*. We calibrated and validated a two-dimensional hydrodynamic model, Hydrologic Engineering Center – River Analysis System (HEC-RAS), at the Wabash and Tippecanoe River confluence with high-resolution bathymetry data for river channels and LiDAR-derived DEM data for the floodplains, which is further described in Dey et al. (2022). We characterized velocity distributions at each sampling location with the median, maximum, and quantiles (10%, 90%, 95%, and 99%) from hourly flood velocity time series across the study period. From an hourly inundation depth time series, we aggregated the total days flooded in the previous 6 months, 3 months, one month, and one week before each sampling date for each sampling location. We also estimated inter-arrival periods as the days since the last flood. If an overbank flooding event did not occur during our period of record, we treated the inter-arrival period as a missing value.

2.3.3. Seasonal Weather Variables

To account for inter-annual variability in seasonal temperature and precipitation, we obtained daily weather data from a nearby National Ocean and Atmospheric Administration National Weather Service Station (USC00129430, 13 km – 18 km from the sites) and aggregated metrics to represent short-term (one day, 2 days, and 7 days before each sampling date) and long-term (one month, 3 months, and 6 months) patterns in precipitation and temperature. Weather metrics included minimum, maximum, and mean daily air and soil temperatures; standard deviation of these daily temperature metrics; and cumulative rainfall, snowfall, and total precipitation.

2.3.4. Vegetation Controls

We completed a vegetation survey by marking the extent of distinct plant communities with a handheld GPS and identifying plant species at each sampling location (5 m vicinity) in October 2019. We continued to assess dominant plant species at each sampling location during subsequent seasonal sampling campaigns: fall 2019, winter 2020, and spring 2020. For survey identification, we used the Seek by iNaturalist mobile application to assist with identifying surveyed vegetation based on photographs (California Academy of Sciences, San Francisco, United States). To address data gaps in vegetation communities before fall 2019, we integrated information from ground-level site photographs and remote sensing approaches to identify or verify the dominant vegetation community at each sampling location during each season before fall 2019. We obtained Sentinel-2 Level-2A and Landsat 8 Operational Land Imager surface reflectance products from the Copernicus Open Access Hub (European Space Agency, Paris, France) and EarthExplorer (United States Geological Survey, Reston, Virginia, United States), respectively. We used our field surveys as training data for the supervised classification of vegetation communities in the ERDAS Imagine remote sensing software package (Hexagon AB, Stockholm, Sweden) based on surface reflectance raster images. We developed vegetation signatures as feature space objects from combinations of spectral bands that provided the most significant differentiation (Laba et al. 2008; Zhou et al. 2021). We integrated information from site photographs, on-the-ground mapping, and classifications from remotely sensed images to identify the dominant vegetation community at each sampling location for each growing season. Classification using remote sensing was consistent with survey observations and classification accuracy for each growing season was consistently high (Supplementary Table S1).

2.4. Statistical Analysis

Our analyses aimed to identify field- and plot-scale environmental properties that explain variability in denitrification potential and contrast restoration design approaches. Potential explanatory variables and DEA rates were transformed as necessary to normalize each variable for all parametric tests, which were evaluated using a threshold of significance of 0.05. DEA_{CN} represents denitrification capacity with ample NO_3^- and organic C, while DEA_{River} represents denitrification under potentially nutrient-limited conditions and simulates rates during an overbank flooding event with ambient river water concentrations. To assess the impact of NO_3^- and organic C limitations of denitrifying microbes

across restoration design strategies and seasons, differences between organic C- and NO_3^--amended rates and ambient rates incubated with river water only were evaluated to generate the ΔDEA values ($\Delta DEA = DEA_{CN} - DEA_{River}$).

We fit linear mixed-effects models to assess seasonality and the impacts of the restoration design approach on DEA_{River}, $DEA_{CN,}$ and ΔDEA with the *lme4* package in R (Bates et al. 2023). Fixed effects included season, site (i.e., WR-A, TR-P, WR-P, and WR-W), and interaction of these variables. The sampling location was incorporated as a random effect. We evaluated the significance of each term with a Type III analysis of variance table (ANOVA) via the Satterthwaite method. If the interaction of season and restoration design approach was not significant, we removed the interaction term from the model. We then estimated the marginal and conditional R^2 of the model and the partial R^2 of the fixed effects with the *partR2* package (Stoffel et al. 2023). For cases when the interaction was significant, we estimated variance attributed to the main effects from a reduced model with the interaction excluded and variance associated with the interaction from the full model. We used the *emmeans* package in R to calculate estimated marginal means for each site and to evaluate all pairwise differences in these estimated marginal means via the Tukey method with the Kenward-Rogers method for degrees of freedom (Lenth et al. 2023). We repeated this approach to evaluate pairwise differences between seasons for DEA_{CN} and DEA_{River} but implemented the Tukey HSD test to contrast ΔDEA to assess the seasonality of nutrient limitations within each floodplain site.

We used boosted regression trees (BRTs) to identify important predictors of DEA_{River} and DEA_{CN}, because BRTs can assess nonlinear and interactive relationships and include quantitative and categorical variables (Elith et al. 2008; Lampa et al. 2014). Before fitting BRTs, we performed correlation analysis and principal component analysis (PCA) with all potential explanatory variables, guiding the reduction of the number of input variables by identifying predictor variables that were highly correlated with each other and variables that were not predictive. The final input variables are presented in Table 1. We used random sampling to generate training and testing datasets for DEA_{River} (n=284) and DEA_{CN} (n=251), which included 85% and 15% of observations, respectively. We fit BRTs to training data for DEA_{River} and DEA_{CN} using *gbm.step* in the *dismo* package with 50-fold cross-validation (Hijmans et al. 2023). We systematically altered the learning rate, tree complexity, and bagging fraction to find the best set of parameters for the model based on the total deviance explained. The final learning rate, tree complexity, and bagging fraction were 0.001, 5, and 0.70, respectively. We made the models more parsimonious by eliminating redundant variables with forward selection via *gbm.simplify* and selected a subset of predictors based on changes in predictive deviance. We evaluated model efficacy by calculating the root mean square error (RMSE) for training and testing datasets and total deviance explained by cross-validation based on methods described by Nieto and Mélin (2017). We tested interactions with *gbm.interactions*, which assesses the strength of second-order interaction effects as the residuals of a linear model of predictor pairs and predicted values based on these pairs.

3. Results

3.1. Denitrification Differed across Restoration Design Approaches and Seasons

$DEA_{River,}$ DEA_{CN}, and ΔDEA varied significantly across sites and seasons ($p < 0.01$, linear mixed-effects models, Table 2). Season and site also had a significant interaction in each model. Prairie and wetland floodplains had different seasonal patterns of denitrification than the agricultural floodplain. These fixed effects and the random effect of sampling location explained 67.7% and 66.5% of the variance in DEA_{River} and DEA_{CN}, respectively (conditional R^2, Table 2).

Variance partitioning revealed that site had the strongest effect on denitrification capacity, accounting for most of the variance explained by each model (partial R^2, Table 2). We found that DEA_{River} and DEA_{CN} were significantly higher in restored floodplain sites (i.e., TR-P, WR-P, WR-W) than in the agricultural floodplain, WR-A ($p < 0.05$, pairwise Tukey contrasts, Figure 2). The mean DEA_{River} in the agricultural floodplain corresponded to less than 20% of the mean rates in the restored floodplains (Table 3, Supplementary Table S4), despite having similar riverine NO_3^- concentrations (Supplementary Table S2). Restored sites also had a larger ΔDEA values, or more severe nutrient limitations, than WR-A (Figure 3, Supplementary Table S4). The wetland floodplain, WR-W, supported higher DEA_{River} than prairie floodplains, although only the difference between the prairie along the Tippecanoe River (TR-P) and WR-W was significant (Table 3, Figure 2A). The prairie floodplain along the Wabash River (WR-P) supported higher mean DEA_{CN} than WR-W, although not significantly, while TR-P had significantly lower DEA_{CN} than WR-P and WR-W (Figure 2B).

Seasonality had a considerably weaker, yet still significant, influence on denitrification capacity than site (Table 2). DEA_{River} was highest during winters, while DEA_{CN} was highest in summers despite incubating

Table 1 Final input variables included as potential predictors of denitrification in boosted regression tree (BRT) models

Variable	Type	Units
Restoration Design Approach	Design and Management	Categorical
Vegetation Community	Vegetation	Categorical
Moisture Content	Soil	% (g/g)
Organic Matter Content	Soil	% (g/g)
Total N Content	Soil	% (g/g)
C:N	Soil	(g/g)
Silt Content	Soil	%
Clay Content	Soil	%
$CaCO_3$ Content	Soil	% (g/g)
Bulk Density	Soil	g/cm^3
Bedrock Type	Soil	Categorical
10^{th} Percentile Flood Velocity	Hydrogeomorphic	ft/s
Maximum Flood Velocity	Hydrogeomorphic	ft/s
Inundation in the Previous Month	Hydrogeomorphic	days
HDND	Hydrogeomorphic	ft
HAND	Hydrogeomorphic	ft
Slope to Nearest Drainage	Hydrogeomorphic	ft/ft
Geomorphic Class	Hydrogeomorphic	Categorical
Total Precipitation in the Previous Month	Seasonal Weather	in
Mean of Maximum Air Temperature in the Previous Month	Seasonal Weather	°F
Season	Seasonal Weather	Categorical

slurries at the same temperature in the laboratory ($p < 0.05$, pairwise Tukey contrasts, Supplementary Table S5). Lack of alignment in the seasonality of DEA_{CN} and DEA_{River} contributed to variation in ΔDEA across seasons (Figure 3). Further investigation of the significant interaction revealed that design approaches had different seasonal patterns in ΔDEA. ΔDEA was consistently near zero in WR-A across seasons, while substrate limitations were typically most severe during the summer in restored floodplains ($p < 0.05$, Tukey HSD test, Figure 3).

Table 2 Summary of linear mixed-effects models for ambient denitrification (DEA_{River}), potential denitrification (DEA_{CN}), and the paired difference between these metrics (ΔDEA). The proportions of variance explained by the overall model (conditional) and fixed effects (marginal) are represented by the coefficient of determinations, R^2. The contributions of each model term to the variance attributed to the fixed effects are represented by partial R^2. We evaluated the significance of each fixed effect, which is summarized by the p-value. Bolded p-values are significant.

Measure	R^2		Fixed Effects	Partial R^2	p-value
DEA_{River}	Conditional	0.677	Site	0.529	**<0.001**
	Marginal	0.584	Season	0.030	**<0.001**
			Site: Season	0.030	**0.002**
DEA_{CN}	Conditional	0.665	Site	0.455	**<0.001**
	Marginal	0.524	Season	0.039	**<0.001**
			Site: Season	0.037	**0.002**
ΔDEA	Conditional	0.256	Site	0.130	**<0.001**
	Marginal	0.227	Season	0.039	**0.005**
			Site: Season	0.062	**0.018**

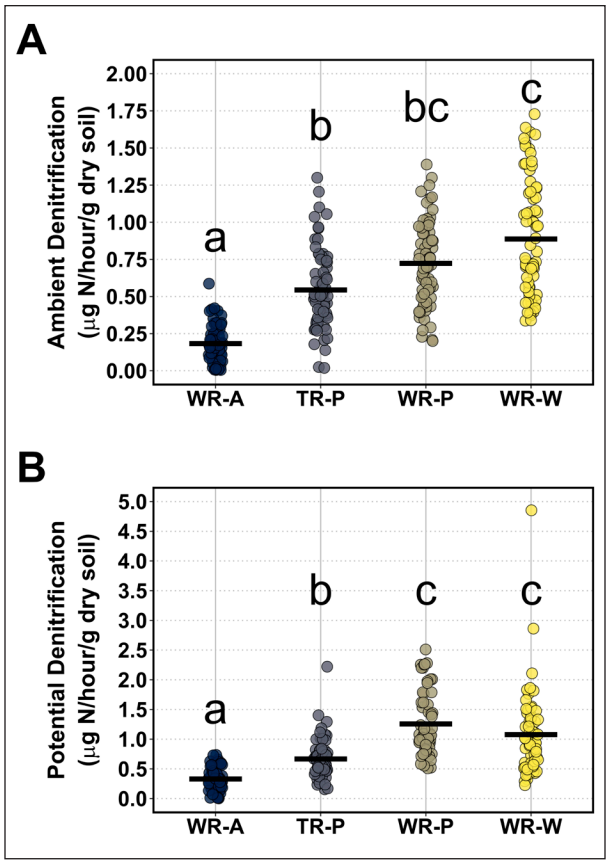

Fig. 2. Jitter plots of denitrification across sites. The black bar represents mean denitrification. Compact letter display designates which sites had comparable denitrification rates such that sharing a letter indicates there was no statistically significant difference between a given site and all other sites that share this letter based on *post hoc* pairwise testing. A.) Ambient denitrification (DEA_{River}) was significantly lower in the agricultural floodplain (WR-A) than in prairie and wetland floodplains. The wetland floodplain (WR-W) supported significantly more ambient denitrification than the prairie along the Tippecanoe River (TR-P), while the prairie along the Wabash River (WR-P) supported intermediate denitrification capacity between the other prairie floodplain and wetland floodplain. B.) Potential denitrification (DEA_{CN}) was significantly lower in the agricultural floodplain than in restored floodplains. The prairie floodplain along the Wabash River (WR-P) and the wetland floodplain had comparable potential denitrification rates. DEA_{CN} is scaled differently from DEA_{River} due to a broader range of values.

3.2. Predictors of Denitrification Potential

Environmental variables, including vegetation type, soil OM, soil $CaCO_3$ content, season, soil moisture content, and total soil N, explained 76.4% of DEA_{River} deviance using a BRT model (Figure 4). The model was highly predictive, with a CV correlation of 0.738±0.034 and RMSE values for testing and training data of 0.29 and 0.19, respectively. Row crops and minimally vegetated areas supported notably less DEA_{River} than native vegetation types (Figure 4A). BRTs featured threshold relationships between DEA_{River} and some soil properties. In each case, DEA_{River} rates did not vary with these soil properties until a threshold was reached. We determined that these minimum thresholds for increases in DEA_{River} were approximately 2.5% for soil OM, 6% for $CaCO_3$ content, and 20% for gravimetric soil moisture content (Figures 4B-C, 4E). We also identified maximum thresholds for these soil properties, such that increases beyond about 10% for soil OM, 7% for $CaCO_3$ content, 40% for soil moisture content, and 0.4% for soil total N were not associated with further increases in DEA_{River} (Figure 4B-C, 4E-F).

Except for the addition of silt content, the DEA_{CN} BRT model (deviance explained: 74.1%, CV correlation: 0.761±0.040) included the same predictors as the DEA_{River} model but had slightly higher error (RMSE of 0.31 and 0.32 for testing and training data, respectively) (Supplementary Figure S5). In both models, vegetation had a considerable impact on denitrification and a significant interaction with soil OM (interaction size: DEA_{CN}=1.00, DEA_{River}=1.60). Amaranth (A), giant ragweed (GR), reed canary grass (RCG), and tall goldenrod (TG) were associated with higher DEA_{River} (Figure 4A) and DEA_{CN} (Supplementary Figure S5A). Further investigation revealed that vegetation with the highest partial dependence also tended to have elevated OM in underlying soils (Supplementary Figure S6A-B). Vegetation also interacted strongly with soil moisture in the DEA_{CN} model (interaction size=5.09, Supplementary Figure S6C), while moisture content interacted with season in the DEA_{River} model (interaction size: 0.65, Supplementary Figure S7). Vegetation categories associated with lower denitrification, including bare soil (BS), soybeans (S), and corn (C), also tended to have lower soil moisture content (Supplementary Figure S6C). Given these interactions, we further investigated the importance of vegetation by fitting BRT models without vegetation as a predictor. We found that the DEA_{River} model without vegetation had comparable explanatory power to the model with vegetation, explaining 76.9% of deviance. $CaCO_3$ content, soil OM, soil moisture content, total soil N, and season were retained as predictors in the DEA_{River} model without vegetation. The design approach (i.e., prairie, agriculture, or wetland) was added as an important predictor. The relative importance of $CaCO_3$ content (11% to 34%) and soil OM (18% to 24%) increased considerably in the model without vegetation. Hydrogeomorphic variables, such as HAND, HDND, flood velocity, and days inundated, were not selected as predictors in any

Table 3 Mean and standard error of denitrification enzyme activity by site. Ambient denitrification (DEA_{River}) number of observations (n): WR-A (agricultural floodplain)=70, TR-P (prairie floodplain on the Tippecanoe River)=71, WR-P (prairie floodplain on the Wabash River)=71, WR-W (wetland floodplain) =72; Potential denitrification (DEA_{CN}) (n): WR-A=62, TR-P=63, WR-P=63, WR-W=63.

Measure	WR-A	TR-P	WR-P	WR-W
DEA_{River} (ambient) (μg N_2O-N/hour/g dry soil)	0.183±0.014	0.544±0.032	0.723±0.033	0.887±0.047
DEA_{CN} (potential) (μg N_2O-N/hour/g dry soil)	0.330±0.023	0.667±0.042	1.256±0.066	1.077±0.089

of the BRT models. Other than flood velocity, hydrogeomorphic variables were not strongly correlated with denitrification rates (Supplementary Table S9).

4. Discussion

Despite excess riverine N export from agricultural production throughout the study sites' watersheds, experiments showed that for all floodplain sites studied, incoming NO_3^- was not high enough to support maximum rates of soil denitrification. This highlights that the capacity of these sites to improve downstream water quality may not be fully realized. Thus, greater annualized N removal can be supported by maximizing hydrologic connectivity and increasing residence times when concentrations of NO_3^- from the river are highest. The positive relationship between soil organic matter and denitrification suggests that organic C availability may further limit denitrification. While we hypothesized that hydrogeomorphic characteristics would emerge as key predictors of denitrification, we noted that denitrification rates had the strongest relationships with soil properties and vegetation. These soil and vegetation properties also helped explain differences in denitrification across sites, such as the floodplain with row crops having lower denitrification potential, less soil organic matter and N, and coarser soil texture than the floodplains with restored native vegetation. Our results indicate that sediment size, increased moisture, and accumulation of organic matter, which are linked to increased floodplain connectivity and restoration of native vegetation, are likely

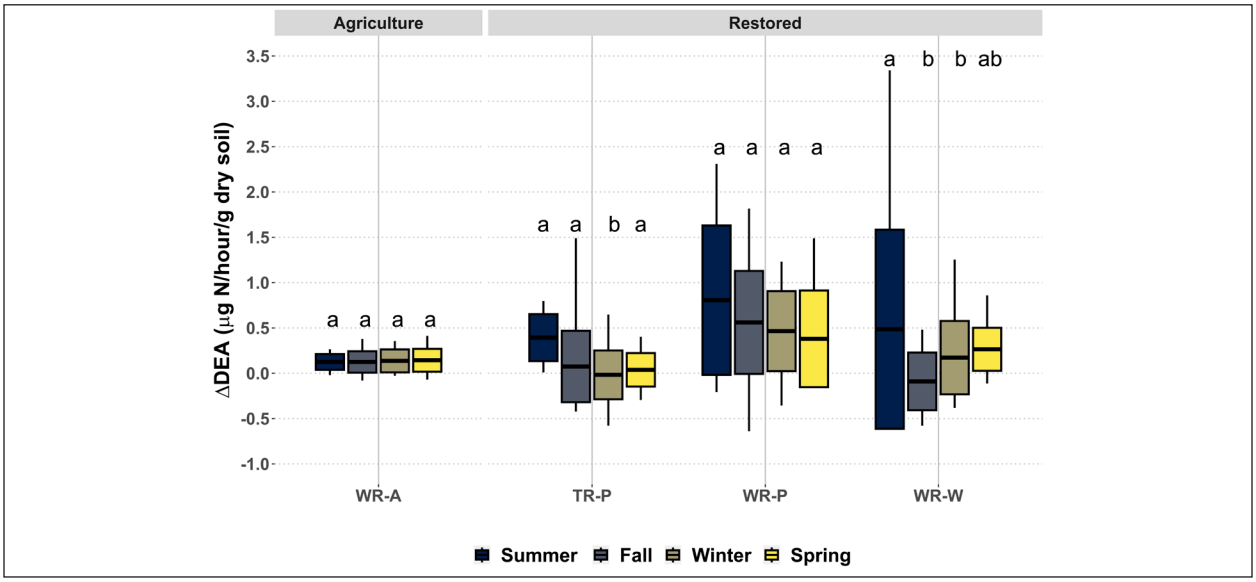

Fig. 3. Boxplots of the paired difference in potential (DEA_{CN}) and ambient (DEA_{River}) denitrification (ΔDEA) across meteorological seasons and floodplain sites (n per site and season: 17-18, except for summer: n=9). The black horizontal bar represents mean values. The edges of the boxes are one standard deviation beyond the mean in either direction. The whiskers represent the maximum and minimum values. The season significantly affected ΔDEA, yet these seasonal effects depended on the restoration design approach. The compact letter display was used to show significant pairwise differences among seasons within each site based on pairwise Tukey tests. Seasons with the same letter are comparable, while seasons without a shared letter are significantly different.

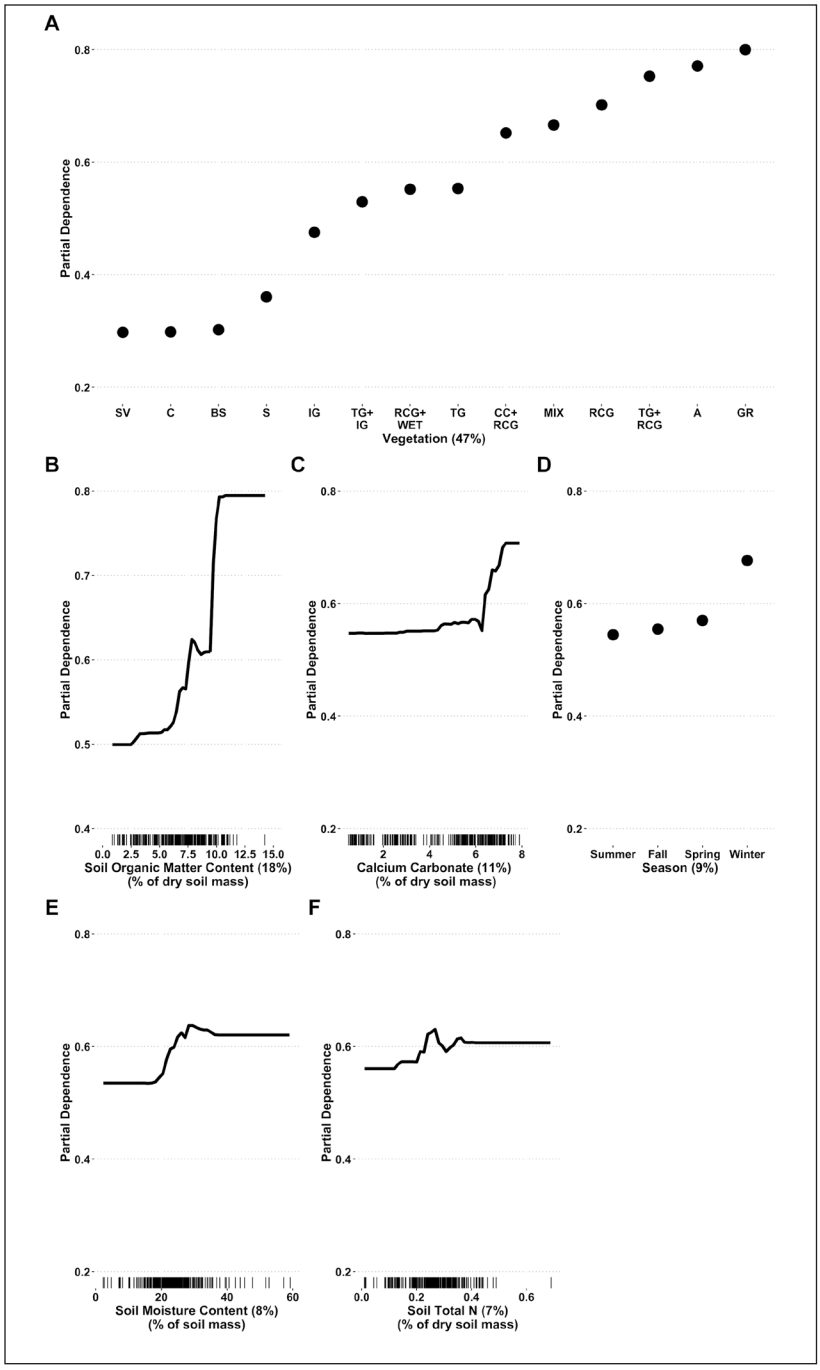

Fig. 4. Boosted regression tree (BRT) partial dependence plots display the marginal effects of significant predictors on ambient denitrification (DEA_{River}). The relative importance of each predictor as a percentage is in parentheses. The x-axis includes rug plots that show the marginal distributions (observation density) of each predictor variable. A.) Vegetation type [SV=sparsely vegetated, C=corn, BS=bare soil, S=soybeans, IG=Indiangrass, TG+IG=tall goldenrod and Indiangrass, RCG+WET=reed canary grass and a mix of obligate wetland plants, TG=tall goldenrod, CC+RCG=cutleaf coneflower and reed canary grass, MIX=mixed shrubs and grasses, RCG=reed canary grass, TG+RCG=tall goldenrod and reed canary grass, A=amaranth, GR=giant ragweed]; B.) Soil organic matter content (OM); C.) Calcium carbonate ($CaCO_3$) content ; D.) Season; E.) Soil moisture; F.) Soil total N.

drivers behind increased denitrification capacity.

4.1. Floodplains are Substrate-Limited

Soil organic matter content and total soil N were positively associated with denitrification rates across design approaches, indicating that floodplain soil denitrification is limited by substrate supply. Our results align with other investigations that found positive relationships between denitrification and supplies of N and organic C in soils or floodwaters (Sheibley et al. 2006; Orr et al. 2007; McMillan and Noe 2017; Korol et al. 2019). The role of substrate supply as a driver of denitrification is further reflected in the seasonality of denitrification rates and ΔDEA, or the difference between denitrification incubated with both labile organic C and NO_3^- additions (DEA_{CN}, or potential denitrification) and with only river water (DEA_{River}). During the growing season, denitrification in samples collected from restored sites appears to be more strongly limited by substrate supply, potentially as warmer temperatures drive higher potential denitrification rates. Lower NO_3^- concentrations during summer months likely led to lower denitrification in samples incubated with river water, resulting in higher ΔDEA. These lower NO_3^- concentrations in the rivers and a lower probability of floodplain inundation during summers suggest that, although warm temperatures may enhance microbial metabolism, there are limited opportunities for soil denitrifying communities to impact riverine water quality significantly during summer.

Despite being situated in N-enriched watersheds, our results indicate that floodplain soil denitrification capacity is not saturated by NO_3^-. Most excess NO_3^- load is exported from late winter to early

spring during high flows from agricultural landscapes in the Mississippi River Basin (Royer et al. 2006). Higher NO_3^- concentrations in river water during winter seemed to stimulate higher denitrification enzyme activity compared to other seasons when river water with lower NO_3^- concentrations was added to soils. NO_3^- supply is influenced by numerous factors, some of which can be controlled through design and management. Thus, this apparent responsiveness of soils in restored floodplains to changes in NO_3^- concentrations implies that restoration designs might increase total N removal in floodplains by frequently routing NO_3^--enriched waters to organic C-enriched soils via placement of restorations downstream of nutrient sources and by increasing hydrologic exchange flows regardless of placement.

4.2. Restoring Floodplains as Wetlands Maximizes Soil Denitrification Potential

Our results suggest that practitioners can design floodplain restorations to include wetlands to maximize reduction of downstream N transport. This finding is consistent with other studies that demonstrate the importance of floodplains and wetlands in particular to target NO_3^- retention in fluvial systems (Forshay and Stanley, 2005, Roley et al. 2012, Wolheim et al. 2014, Hanrahan et al. 2018). These studies identified higher soil organic matter (Roley et al. 2012) and greater water residence time (Wolheim et al. 2014) as key elements driving increased uptake of NO_3^-. Both soil conditions and water residence time are key. When floodplain wetland restorations were situated in areas where water residence time is low, for example in smaller streams and rivers, NO_3^- retention was reduced (Jones et al. 2015). We measured the highest denitrification rates using river water in the wetland floodplain where hydrologic connectivity was estimated to be greatest in terms of frequency of overbank flooding and restored wetland hydrology (Supplementary Table S3; Supplementary Figure S2). The wetland floodplain supported more than 20% and 60% higher mean denitrification rates than the prairie floodplains when incubated with river water. Hansen et al. (2018) similarly found that restoring wetlands should remove 5 times more NO_3^- than placing the same amount of land into conservation. Consistent with this previous work, we found that greater modification of floodplain structure to increase wetland attributes, such as greater hydrologic connectivity and water residence time, can support higher denitrification than just converting land from agricultural production into conservation (i.e., only planting native vegetation). Our finding that concentrations of NO_3^- limit denitrification rates in floodplain restorations is also consistent with previous work (Orr et al. 2007, Roley et al. 2012).

While denitrification with river water was highest in the wetland floodplain, mean organic C and NO_3^--amended denitrification rates in the prairie along the Wabash River were comparable to rates in the wetland floodplain. Soils with some of the highest amended denitrification rates in this prairie floodplain were sampled within and near a seepage wetland at the transition between upland and floodplain ecosystems. These sampling locations also had elevated soil organic matter and the most considerable differences between denitrification with organic C- and NO_3^--amendments versus river water, leading us to posit that persistent contact between upper soil horizons and groundwater seems to have supported microbial communities that had already depleted available soil NO_3^- and were primed to treat additional incoming NO_3^-. This high capacity to treat N in wetlands with strong groundwater connections has been attributed to extended residence times in other studies (Harrison et al. 2014). The high denitrification capacity associated with this minor wetland feature in the prairie floodplain further highlighted that restoring wetland areas in floodplains, especially groundwater-fed wetlands, is key if denitrification is a primary goal of restoration.

Enhanced hydrologic connectivity likely supported soil conditions that favored denitrification. The wetland floodplain and prairie floodplain along the Wabash River, which had the highest amended denitrification rates, also had higher soil moisture than other sites. These wetland areas had persistently moist soils due to ponding or saturation at the soil surface that persisted into the growing season. These sites also had considerably higher $CaCO_3$ content. Shallower water tables, such as those in the wetland floodplain and seepage wetland, can lead to a build-up of salts, such as carbonates, near the soil surface. Therefore, the predictive power of $CaCO_3$ may reflect the coincidence of higher subsurface hydrologic connectivity and denitrification rates. Alternatively, higher $CaCO_3$ may reflect higher deposition of carbonate-enriched sediments from more frequent flooding, as bedrock in the contributing watersheds is mainly limestone, dolomite, shale, and sandstone (USACE 2011). Furthermore, pH increases with increasing $CaCO_3$ content, and Kaden et al. (2021) found that soil pH was a strong predictor of denitrification potential in floodplain soils. Yet, we did not find a strong relationship between soil pH and $CaCO_3$ content for a subset of seasonal sampling campaigns.

4.3. Vegetation Types Predict Denitrification Capacity

We observed clear differences in denitrification capacity across soils underlying different vegetation species. Such differences in denitrification across vegetation

types are frequently observed in riparian and wetland ecosystems (Seitzinger et al. 2006; Alldred and Baines 2016), but the degree to which plant species is a driver of higher denitrification rates versus simply an indicator of soil conditions that are more conducive to denitrification is unclear. We noted similar explanatory power of boosted regression tree models with and without vegetation type as a predictor. This is because vegetation type covaries with soil properties that are key predictors of denitrification, particularly soil organic matter and moisture. If specific plant characteristics can be linked to both differences in denitrification and soil conditions across vegetation types, practitioners may be able to increase denitrification in restored floodplains by incorporating vegetation with these desirable characteristics in their planting plans. Such relationships create connections between soil conditions and planting design, which is actionable from an ecological engineering perspective.

Our results suggest that selecting plants that efficiently contribute bioavailable organic matter to soils can support higher denitrification. Amaranth, reed canary grass, and giant ragweed had both high denitrification potential and soil organic matter in underlying soils. Amaranth and giant ragweed are annuals, likely contributing sizable amounts of detritus to soils upon senescence. Reed canary grass is a perennial but has been reported to have more easily decomposable litter and to support higher concentrations of water-extractable organic C in underlying soils than woolgrass (*Scirpus cyperinus*) and mixtures of non-invasive, native plants in other wetlands in the Wabash River Basin (Bills et al. 2010). The alignment between vegetation, soil organic matter, and denitrification rates also likely reflects the impacts of design approach, particularly differences in land use, on both soil conditions and vegetation. We observed that only a few vegetation communities were present across multiple sites. Vegetation types (i.e., sparse ground cover, bare soil, soybeans, and corn) that supported the lowest denitrification potential were exclusively found within the agricultural floodplain, which had coarser and drier soils with less organic matter and soil N than restored sites. Harvesting represents a key management difference between these agricultural vegetation communities associated with low denitrification and native vegetation communities in other sites, where more biomass is available to contribute to the development of soil organic matter.

Soil moisture may further explain links between vegetation and denitrification across design approaches. Vegetation is often used to indicate long-term soil moisture regimes in wetlands and floodplains based on different tolerances for saturation and inundation (Whited et al. 2007). Amaranth and giant ragweed, which had the highest denitrification rates with river water, were solely mapped in the wetland floodplain. Amaranth is considered an obligate wetland plant in the Midwest, and giant ragweed is a facultative wetland plant such that the interaction of soil moisture and vegetation in our study may also reflect the tendencies of amaranth and giant ragweed to thrive in wetter portions of the floodplain and of denitrification to be heightened in moist soils (USACE 2010). By contrast, Indiangrass and tall goldenrod are facultative upland and facultative wetland species, respectively, indicating a preference for drier soil than amaranth and giant ragweed (USACE 2010). The soils underlying these vegetation types had significantly lower soil moisture than other plant communities within the same floodplain, and these species were also associated with lower denitrification rates.

Our results underscore the importance of vegetation but also highlight the need to outline mechanistic links between vegetation and denitrification in restored floodplain ecosystems. Specifically, our work identified knowledge gaps regarding how plants regulate soil redox conditions and the lability of soil organic matter. Using more controlled experimental approaches to understand why certain plants support higher denitrification and identifying specific plant properties, such as basal area or hemicellulose content of litterfall, that enhance denitrification potential can make findings more translatable across plant types. Incorporating vegetation with characteristics associated with high denitrification into restoration provides a straightforward approach for practitioners to manage soil characteristics. Relationships between certain soil properties and denitrification are well-established, but soil properties are more difficult to characterize and monitor with remote sensing and field visits than vegetation. Given the strong links we identified between plant community and soil properties, vegetation type may be a useful surrogate to inexpensively screen for denitrification hotspots in riverine floodplains.

4.4. The Farmed Floodplain Provided Limited Water Quality Benefits

Our results suggest that using seasonally flooded floodplains for row crop agriculture may support notably lower denitrification capacity than replanting floodplains with native vegetation, as the agricultural floodplain had lower denitrification rates than restored floodplains despite being flooded for more days annually than prairie floodplains during the project period. Soil conditions that were associated with lower denitrification rates across our sites (e.g., depleted total N, limited

soil organic matter content, reduced soil moisture, and higher sand content) were characteristic of this agricultural floodplain. This floodplain was managed using conventional farming practices, including tillage, fertilization, and leaving soils relatively exposed during winter and spring floods. Mean soil organic matter content (3.9% versus 7.5%) and total soil N (0.13% versus 0.29%) were significantly lower in the agricultural than the restored floodplains, which may be driven by limited detrital inputs and higher erosion risk from harvesting and tilling. While we do not have detailed information on fertilization rates, the low rates of denitrification we documented suggest that applied N not used by crops would be exported.

Coarser soil texture in the agricultural floodplain may have also constrained denitrification capacity. Agricultural operations in this floodplain might have shifted soil textures. For instance, reduced surface resistance during flooding from leaving soils more exposed outside of the growing season may have altered erosion and deposition patterns compared to the restored floodplains. Alternatively, this site may have been preferentially selected to be farmed rather than restored with native vegetation due to coarser soils that promote more rapid drainage to support crop production. Grain size distribution consistently predicts spatial and temporal variability in floodplain denitrification (Pinay et al. 2000; Hoagland et al. 2019). Coarse soils have lower capacities to retain water, N, and organic C, which likely further explain reduced soil N, organic matter, and moisture levels in the agricultural floodplain, thereby limiting denitrification potential (Pinay et al. 1995; Pinay et al. 2000). Low organic matter accumulation in wetlands converted from farming has previously been associated with low denitrification potential after restoration, particularly with elevated sand content (Ballantine et al. 2017).

Analysis of ΔDEA revealed that denitrification remains low in the agricultural site even when additions of organic C and NO_3^- ameliorate substrate limitations. More abundant labile organic C and anaerobic microsites in finer textured soils are needed to drive higher denitrification rates but also to support the development of active denitrifying communities that can respond when environmental conditions become favorable, such as during overbank flooding events that replenish NO_3^- (Calderer et al. 2014; Deslippe et al. 2014; Chen et al. 2023). This muted response to substrate additions suggests that agricultural soils in our study may have lacked robust denitrifying communities. Orr et al. (2007) similarly hypothesized that deficits in denitrifying communities might explain low denitrification potential in previously farmed floodplains.

4.5. Different Metrics for Hydrologic Connectivity are Needed to Inform Design and Management

We found indirect evidence to support our hypothesis that hydrogeomorphic characteristics would explain variability in denitrification. Specifically, we identified indirect evidence of the role of hydrogeomorphology on modulating denitrification. For instance, we measured the highest denitrification rates in the wetland floodplain and the most hydrologically connected geomorphic features. We also found that soil properties that are regulated by hydrogeomorphic characteristics and processes, including moisture, organic matter, and texture, effectively predicted denitrification. Yet, quantitative metrics that directly measure hydrologic connectivity, including HAND, HDND, flood velocity, and days inundated, were not strong predictors of denitrification. Thus, our work suggests that model outputs from HEC-RAS and connectivity metrics derived from digital elevation models, including HAND, do not as effectively capture the hydrogeomorphic processes and properties most relevant to denitrification as did the measured soil properties. Kaden et al. (2021) also found that certain soil properties were better predictors of floodplain denitrification potential than hydrologic parameters despite the hydrologic regime seeming to still be a key driver of denitrification capacity. We observed the persistence of shallow water tables in portions of the wetland floodplain well into the summer. However, only analyzing the time series of inundation depth from HEC-RAS would suggest that this site was much drier during periods of surface disconnection. The seepage wetland in the prairie was saturated or inundated by groundwater throughout the year. Still, days inundated based on the HEC-RAS model suggest that these locations are dry nearly year-round. HEC-RAS is likely the best modeling tool to characterize surface water connections and flood extent in floodplains but does not provide insight into these groundwater connections. Neglecting groundwater connections may have underestimated the overall degree of connectivity of primarily groundwater-fed geomorphic features, thereby limiting the explanatory power of hydrologic connectivity metrics included in our study. The extent of the 100-year floodplain has been identified as another connectivity metric that may not reflect hydrologic processes most relevant to denitrification, as floodplains designated as 'active' may be flooded quite infrequently (Kaden et al. 2023).

HEC-RAS also does not provide insight into residence time. We anticipate that residence time will further explain denitrification rates. Without a persistent surface connection, the seepage wetland in the prairie floodplain likely had uncharacteristically high residence times

compared to other sampling locations. Floodwater was also trapped in ephemeral channels and backwater areas of floodplains for extended periods after floods receded, and these low-lying geomorphic features often supported elevated denitrification potential. Other studies have successfully used residence times to explain variation in denitrification rates, particularly when contrasting surface water and groundwater connections (Harrison et al. 2014; Kjellin et al. 2007). We recommend using tightly coupled surface water-groundwater models or field monitoring to better characterize the surface and subsurface hydrologic connections and develop quantitative predictors of denitrification capacity that represent hydrogeomorphic conditions.

Spatial resolution issues may further explain why these modeled hydrogeomorphic variables were not strong predictors of denitrification. Local variations in soil moisture due to slight differences in elevation are likely not discernible in model outputs. Greater microtopography has been linked to higher denitrification capacity by encouraging the formation of neighboring aerobic and anaerobic micro-sites that increase closely coupled nitrification-denitrification (Groffman and Tiedje 1988; Wolf et al. 2011). The spatial resolution of our digital elevation model could not capture this fine-scale microtopography, which may have further demurred quantitative links between hydrologic connectivity and denitrification capacity.

5. Conclusion

Understanding the plot- and field-scale predictors of denitrification can inform the design and management of riverine floodplain restorations that efficiently remove N from surface and groundwater. Soil organic matter content and total N were important predictors of denitrifying capacity, and we found that soils in restored floodplains were seasonally limited by substrate availability, particularly riverine NO_3^- supply. We determined that denitrification capacity was substantially lower in the agricultural floodplain than in restored floodplains. The agricultural floodplains in our study also had lower soil organic matter content and total N and coarser soils, which likely impeded the development of robust denitrifying communities.

Vegetation tracked with both denitrification rates and soil properties across design approaches and hydrogeomorphic features. We also determined that a greater degree of hydrologic connectivity with surface waters or groundwater likely enhances denitrification capacity based on the co-occurrence of high denitrification within wetland areas, such as in the wetland floodplain and the seepage wetland within a prairie floodplain. Yet, the hydrogeomorphic metrics derived from elevation and surface water hydrodynamic models, including HAND and cumulative days flooded, for this investigation were not strong predictors of denitrification. Other hydrogeomorphic metrics, which better reflect surface and subsurface connection at higher spatial resolutions, are likely necessary to predict denitrification more accurately and, by extension, guide restoration practitioners in restoring the optimal degree and type of hydrologic connectivity.

Supplementary Material

The online version of this manuscript contains a link to supplementary material that includes: Figure S1: Detailed site maps and site photographs; Table S1: Classification accuracy of remotely sensed vegetation data; Table S2: Water chemistry of river water samples; Table S3: Cumulative days of inundation; Table S4: *Post hoc* pairwise testing by site; Table S5: *Post hoc* pairwise testing by season; Table S6: Mean and standard error of ambient (DEA_{River}) and potential (DEA_{CN}) denitrification by restoration design approach; Figure S2: Time series of river discharge and indicators of inundation discharge; Figure S3: Boxplots of denitrification enzyme activity parsed by the season and year; Figure S4: Bivariate relationships between ambient denitrification rates (DEA_{River}) and quantitative soil variables that were included in the boosted regression tree model of DEA_{River}; Figure S5: Partial dependence plot of the boosted regression tree model of potential denitrification (DEA_{CN}); Figure S6: Boxplots to explore interactions between vegetation and soil properties in the boosted regression tree models; Figure S7: Boxplots of soil moisture content across season using median and interquartile range; Table S7: Correlation tests of denitrification rates with soil properties; Table S8: Mean and standard error of soil properties by site across seasons; Table S9: Correlation tests of hydrogeomorphic properties with denitrification rates; Table S10: Mean and standard error of hydrogeomorphic properties by site across seasons.

Acknowledgments

This work would not have been possible without the contributions of Amanda Limiac, Shannon Donohue, Jonathan Mills, and Ariana Montoya Lozano to field and laboratory work. We would also like to thank the staff at Prophetstown State Park, Purdue University's Agricultural and Biological Engineering program, and the National Soil Erosion Research Laboratory for their assistance throughout the project. The lead author also thanks Sara McMillan, Jacob Hosen, Gregory Noe, Michael Burchell, and Laura Bowling for their guidance and support as members of her Ph.D. committee.

This study was funded primarily by the National Science Foundation (Award Number: 1706612). This material is based upon work supported by the National Science Foundation Graduate Research Fellowship under Grant No. 1842166. Any use of trade, firm, or product names is for descriptive purposes only and does not imply endorsement by the U.S. Government.

Author Contributions Statement

Conceptualization: SWM, GBN, DWL; methodology: SWM, GBN, DWL, SD, JDH; data analysis: DWL, SD; laboratory analyses: DWL; writing original draft: DWL; review/editing original draft: DWL, SWM, JDH; investigation: SWM, GBN; resources: SWM; data curation: DWL, SD; supervision: SWM, JDH; project administration: SWM; funding acquisition: SWM, GBN, DWL.

All authors have read and agreed to the published version of the manuscript.

Conflict of Interest Statement

The authors have no conflict of interest to report.

Data Availability Statement

Data from this study is published online via the Purdue University Research Repository: https://doi.org/10.4231/AAD7-2B97.

Related Publication Statement

This material was previously disseminated as a chapter in Danielle Lay's dissertation.

Citation:

Lay D. 2023. Optimizing design and management of restored wetlands and floodplains in agricultural watersheds for water quality [dissertation]. Purdue University Graduate School. https://doi.org/10.25394/PGS.24749307.v1

References

Alldred M, Baines SB. 2016. Effects of wetland plants on denitrification rates: a meta-analysis. Ecol Appl. 26(3):676–685. https://doi.org/10.1890/14-1525

Atkinson J, Bonser SP. 2020. "Active" and "passive" ecological restoration strategies in meta-analysis. Restor Ecol. 28(5):1032-1035. https://doi.org/10.1111/rec.13229

Ballantine KA, Anderson TR, Pierce EA, Groffman PM. 2017. Restoration of denitrification in agricultural wetlands. Ecol Eng. 106:570–577. https://doi.org/10.1016/j.ecoleng.2017.06.033

Bates D, Maechler M, Bolker B, Walker S, Bojesen Christensen RH. 2023. lme4: Linear Mixed-Effects Models using "Eigen" and S4 (1.1-34). https://cran.r-project.org/web/packages/lme4/index.html

Bernot MJ, Dodds WK, Gardner WS, McCarthy MJ, Sobolev D, Tank JL. 2003. Comparing denitrification estimates for a Texas estuary by using acetylene inhibition and membrane inlet mass spectrometry. Appl Environ Microbiol. 69(10):5950–5956. https://doi.org/10.1128/AEM.69.10.5950-5956.2003

Bills JS, Jacinthe P-A, Tedesco LP. 2010. Soil organic carbon pools and composition in a wetland complex invaded by reed canary grass. Biol Fertil Soils. 46(7):697–706. https://doi.org/10.1007/s00374-010-0476-6

Calderer M, Martí V, de Pablo J, Guivernau M, Prenafeta-Boldú FX, Viñas M. 2014. Effects of enhanced denitrification on hydrodynamics and microbial community structure in a soil column system. Chemosphere. 111:112–119. https://doi.org/10.1016/j.chemosphere.2014.03.033

Chen C, Liu P, Liu Y, Wei Y, Li J, Ding G. 2023. Carbon amendment rather than nitrate fertilization dominated the reassembly of the total, denitrifying, and DNRA bacterial community in the anaerobic subsoil. J Soils Sediments. 23(4):1913–1926. https://doi.org/10.1007/s11368-023-03424-y

Cheng FY, Van Meter KJ, Byrnes DK, Basu NB. 2020. Maximizing US nitrate removal through wetland protection and restoration. Nature. 588:625-630. https://doi.org/10.1038/s41586-020-03042-5

Clilverd HM, Thompson JR, Heppell CM, Sayer CD, Axmacher JC. 2016. Coupled hydrological/hydraulic modeling of river restoration impacts and floodplain hydrodynamics. River Res Appl. 32(9):1927–1948. https://doi.org/10.1002/rra.3036

Deslippe JR, Jamali H, Jha N, Saggar S. 2014. Denitrifier community size, structure and activity along a gradient of pasture to riparian soils. Soil Biol Biochem. 71:48–60. https://doi.org/10.1016/j.soilbio.2014.01.007

Dey S, Saksena S, Winter D, Merwade V, McMillan S. 2022. Incorporating network scale river bathymetry to improve characterization of fluvial processes in flood modeling. Water Resour Res, 58(11). https://doi.org/10.1029/2020WR029521

Elith J, Leathwick JR, Hastie T. 2008. A working guide to boosted regression trees. J Anim Ecol. 77(4):802–813. https://doi.org/10.1111/j.1365-2656.2008.01390.x

Evenson GR, Golden HE, Christensen JR, Lane CR, Rajib A, D'Amico E, et al. 2021. Wetland restoration yields dynamic nitrate responses across the Upper Mississippi River Basin. Environ Res Commun. 3(9):1–10. https://doi.org/10.1088/2515-7620/ac2125

Federman CE, Scott DT, Hester ET. 2023. Impact of floodplain and Stage 0 stream restoration on flood attenuation and floodplain exchange during small frequent storms. J Am Water Resour As. 59(1):29–48. https://doi.org/10.1111/1752-1688.13073

Forshay KJ, Stanley EH. 2005. Rapid nitrate loss and denitrification in a temperate river floodplain. Biogeochemistry. 75(1):43-64. https://doi.org/10.1007/s10533-004-6016-4

Galloway JN, Dentener FJ, Karl DM, Michaels AF, Porter JH, Townsend AR, et al. 2004. Nitrogen Cycles: Past, Present, and Future. Biogeochemistry. 70(2):153–226. https://doi.org/10.1007/s10533-004-0370-0

García AM, Alexander RB, Arnold JG, Norfleet L, White MJ, Robertson DM, et al. 2016. Regional effects of agricultural conservation practices on nutrient transport in the Upper Mississippi River Basin. Environ Sci Technol. 50(13):6991–7000. https://doi.org/10.1021/acs.est.5b03543

Groffman PM, Holland EA, Myrold DA, Robertson GP, Zou X. 1999. Denitrification. In: Robertson GP et al, editors. Standard soil methods for long-term ecological research. Oxford University Press. p 272–290. https://doi.org/10.1093/oso/9780195120837.003.0014

Groffman PM, Tiedje JM. 1988. Denitrification hysteresis during wetting and drying cycles in soil. Soil Sci Soc Am J. 52(6):1626–1629. https://doi.org/10.2136/sssaj1988.03615995005200060022x

Guida RJ, Remo JW, Secchi S. 2016. Tradeoffs of strategically reconnecting rivers to their floodplains: The case of the Lower Illinois River (USA). Sci Total Environ. 572:43–55. https://doi.org/10.1016/j.scitotenv.2016.07.190

Hanrahan BR, Tank JL, Dee MM, Trentman MT, Berg EM, McMillan SK. 2018. Restored floodplains enhance denitrification compared to naturalized floodplains in agricultural streams. Biogeochemistry. 141:419-437. https://doi.org/10.1007/s10533-018-0431-4

Hansen AT, Dolph CL, Foufoula-Georgiou E, Finlay JC. 2018. Contribution of wetlands to nitrate removal at the watershed scale. Nat Geosci. 11(2):127–132. https://doi.org/10.1038/s41561-017-0056-6

Harrison MD, Miller AJ, Groffman PM, Mayer PM, Kaushal SS. 2014. Hydrologic controls on nitrogen and phosphorous dynamics in relict oxbow wetlands adjacent to an urban restored stream. J Am Water Resour As. 50(6):1365–1382. https://doi.org/10.1111/jawr.12193

Harvey J, Gomez-Velez J, Schmadel N, Scott D, Boyer E, Alexander R, et al. 2018. How Hydrologic connectivity regulates water quality in river corridors. J Am Water Resour As. 55(2): 369-381. https://doi.org/10.1111/1752-1688.12691

Heine RA, Pinter N. 2012. Levee effects upon flood levels: an empirical assessment. Hydrological Processes. 26(21):3225–3240. https://doi.org/10.1002/hyp.8261

Heiri O, Lotter AF, Lemcke G. 2001. Loss on ignition as a method for estimating organic and carbonate content in sediments: reproducibility and comparability of results. J Paleolimnology. 25(1):101–110. https://doi.org/10.1023/A:1008119611481

Hijmans R, Phillips S, Leathwick J, Elith J. 2023. Package "dismo." https://cran.r-project.org/web/packages/dismo/dismo.pdf

Hoagland B, Schmidt C, Russo TA, Adams R, Kaye J. 2019. Controls on nitrogen transformation rates on restored floodplains along the Cosumnes River, California. Sci Total Environ. 649:979–994. https://doi.org/10.1016/j.scitotenv.2018.08.379

Jarrell WM, Armstrong DE, Grigal DF, Kelly EF, Monger HC, Wedin DA. 1999. Soil water and temperature status. In: Robertson GP et al, editors. Standard soil methods for long-term ecological research. Oxford University Press. p 55-73. https://doi.org/10.1093/oso/9780195120837.003.0003

Jaynes DB, Isenhart TM. 2014. Reconnecting tile drainage to riparian buffer hydrology for enhanced nitrate removal. J Environ Qual. 43(2):631–638. https://doi.org/10.2134/jeq2013.08.0331

Jones CN, Scott DT, Guth C, Hester ET, Hession WC. 2015. Seasonal variation in floodplain biogeochemical processing in a restored headwater stream. Environ Sci Technol. 49(22):13190-13198. https://doi.org/10.1021/acs.est.5b02426

Jones HP, Jones PC, Barbier EB, Blackburn RC, Rey Benayas JM, Holl KD, et al. 2018. Restoration and repair of Earth's damaged ecosystems. Proceedings of the Royal Society B, Biological Sci. 285(1873):1-8. https://doi.org/10.1098/rspb.2017.2577

Junk WJ, Bayley PB, Sparks RE. 1989. The flood pulse concept in river-floodplain systems. In: Dodge DP, editor. Proceedings of the International Large River Symposium. Can Spec Publ Fish Aquat Sci. 106:110–127.

Kaden US, Fuchs E, Geyer S, Hein T, Horchler P, Rupp H, et al. 2021. Soil characteristics and hydromorphological patterns control denitrification at floodplain scale. Front Earth Sci. 9:708707. https://doi.org/10.3389/feart.2021.708707

Kaden US, Schulz-Zunkel C, Fuchs E, Horchler P, Kasperidus HD, de Moraes Bonilha O, et al. 2023. Improving an existing proxy-based approach for floodplain denitrification assessment to facilitate decision making on restoration. Sci Total Environ. 892:164727. https://doi.org/10.1016/j.scitotenv.2023.164727

Kjellin J, Hallin S, Wörman A. 2007. Spatial variations in denitrification activity in wetland sediments explained by hydrology and denitrifying community structure. Water Resour. 41(20):4710–4720. https://doi.org/10.1016/j.watres.2007.06.053

Korol AR, Noe GB, Ahn C. 2019. Controls of the spatial variability of denitrification potential in nontidal floodplains of the Chesapeake Bay watershed, USA. Geoderma. 338:14–29. https://doi.org/10.1016/j.geoderma.2018.11.015

Laba M, Downs R, Smith S, Welsh S, Neider C, White S, et al. 2008. Mapping invasive wetland plants in the Hudson River National Estuarine Research Reserve using Quickbird satellite imagery. Remote Sens Environ. 112(1):286–300. https://doi.org/10.1016/j.rse.2007.05.003

Lampa E, Lind L, Lind PM, Bornefalk-Hermansson A. 2014. The identification of complex interactions in epidemiology and toxicology: a simulation study of boosted regression trees. Environ Health. 13(1):57. https://doi.org/10.1186/1476-069X-13-57

Lenth RV, Bolker B, Buerkner P, Giné-Vázquez, I, Herve M, Jung M, et al. 2023. emmeans: Estimated marginal means, aka least-squares means (1.8.8) https://cran.r-project.org/web/packages/emmeans/index.html

Li S, Twilley RR. 2021. Nitrogen dynamics of inundated sediments in an emerging coastal deltaic floodplain in Mississippi River Delta using isotope pairing technique to test response to nitrate enrichment and sediment organic matter. Estuaries and Coasts. 44(7):1899–1915. https://doi.org/10.1007/s12237-021-00913-6

Liu W, Liu G, Zhang Q. 2011. Influence of vegetation characteristics on soil denitrification in shoreline wetlands of the Danjiangkou Reservoir in China. CLEAN – Soil, Air, Water. 39(2):109–115. https://doi.org/10.1002/clen.200900212

Lutz SR, Trauth N, Musolff A, Van Breukelen BM, Knöller K, Fleckenstein JH. 2020. How important is denitrification in riparian zones? Combining end-member mixing and isotope modeling to quantify nitrate removal from riparian groundwater. Water Resour Res. 56(1):e2019WR025528. https://doi.org/10.1029/2019WR025528

McMillan SK, Noe GB. 2017. Increasing floodplain connectivity through urban stream restoration increases nutrient and sediment retention. Ecol Eng. 108(PA):284–295. https://doi.org/10.1016/j.ecoleng.2017.08.006

Naiman RJ, Decamps H. 1997. The ecology of interfaces: riparian zones. Ann Rev Ecol Syst. 28:621. https://doi.org/10.1146/annurev.ecolsys.28.1.621

Natho S, Tschikof M, Bondar-Kunze E, Hein T. 2020. Modeling the effect of enhanced lateral connectivity on nutrient retention capacity in large river floodplains: How much connected floodplain do we need? Front Environ Sci. 8. https://doi.org/10.3389/fenvs.2020.00074

Nieto K, Mélin F. 2017. Variability of chlorophyll-a concentration in the Gulf of Guinea and its relation to physical oceanographic variables. Progress in Oceanography, 151: 97–115. https://doi.org/10.1016/j.pocean.2016.11.009

Noe G, Hopkins K, Claggett P, Schenk E, Metes M, Ahmed L, et al. 2022. Streambank and floodplain geomorphic change and contribution to watershed material budgets. Environ Res Lett. 17:064015. https://doi.org/10.1088/1748-9326/ac6e47

Noe G, Hupp C. 2005. Carbon, nitrogen, and phosphorus accumulation in floodplains of Atlantic Coastal Plain Rivers, USA. Ecol Appl. 15(4):1178–1190. https://doi.org/10.1890/04-1677

Noe GB, Hupp CR. 2009. Retention of riverine sediment and nutrient loads by coastal plain floodplains. Ecosystems (New York). 12(5):728–746. https://doi.org/10.1007/s10021-009-9253-5

Olde Venterink H, Vermaat JE, Pronk M, Wiegman F, Lee GEM, Hoorn MW, et al. 2006. Importance of sediment deposition and denitrification for nutrient retention in floodplain wetlands. Appl Veg Sci. 9(2):163–174. https://doi.org/10.1111/j.1654-109X.2006.tb00665.x

Opperman JJ, Galloway GE, Fargione J, Mount JF, Richter BD, Secchi S. 2009. Land use. Sustainable floodplains through large-scale reconnection to rivers. Science (American Association for the Advancement of Science). 326(5959):1487–1488. https://doi.org/10.1126/science.1178256

Orr CH, Stanley EH, Wilson KA, Finlay JC. 2007. Effects of restoration and reflooding on soil denitrification in a leveed midwestern floodplain. Ecol Appl. 17(8):2365–2376. https://doi.org/10.1890/06-2113.1

Pinay G, Black VJ, Planty-Tabacchi AM, Gumiero B, Décamps H. 2000. Geomorphic control of denitrification in large river floodplain soils. Biogeochemistry. 50(2):163–182. https://doi.org/10.1023/A:1006317004639

Pinay G, Black VJ, Planty-Tabacchi AM, Gumiero B, Décamps H. 1995. Nitrogen cycling in two riparian forest soils under different geomorphic conditions. Biogeochemistry. 30(1):9–29. https://doi.org/10.1007/BF02181038

Quine TA, Cressey EL, Dungait JAJ, De Baets S, Meersmans J, Jones MW, et al. 2022. Geomorphically mediated carbon dynamics of floodplain soils and implications for net effect of carbon erosion. Hydrol Process. 36(9):e14657. https://doi.org/10.1002/hyp.14657

Rajib A, Zheng Q, Golden HE, Wu Q, Lane CR, Christensen JR, et al. 2021. The changing face of floodplains in the Mississippi River Basin detected by a 60-year land use change dataset. Sci Data. 8(1):271. https://doi.org/10.1038/s41597-021-01048-w

Reddy KR, DeLaune RD. 2008. Biogeochemistry of Wetlands: Science and Applications. CRC Press. https://doi.org/10.1201/9780203491454

Roley SS, Tank JL, Stephen ML, Johnson LT, Beaulieu JJ, Witter JD. 2012. Floodplain restoration enhances denitrification and reach-scale nitrogen removal in an agricultural stream. Ecol Appl. 22(1):281–297. https://doi.org/10.1890/11-0381.1

Royer TV, David MB, Gentry LE. 2006. Timing of riverine export of nitrate and phosphorus from agricultural watersheds in Illinois: Implications for reducing nutrient loading to the Mississippi River. Environ Sci Tech. 40(13):4126–4131. https://doi.org/10.1021/es052573n

Salk K, Steinman A, Ostrom N. 2018. Wetland restoration and hydrologic reconnection result in enhanced watershed nitrogen retention and removal. Wetlands. 38(2):349–359. https://doi.org/10.1007/s13157-017-0972-7

Seitzinger S, Harrison JA, Böhlke JK, Bouwman AF, Lowrance R, Peterson B, et al. 2006. Denitrification across landscapes and waterscapes: A synthesis. Ecol Appl. 16(6):2064–2090. https://doi.org/10.1890/1051-0761(2006)016[2064:DALAWA]2.0.CO;2

Sheibley R, Ahearn D, Dahlgren R. 2006. Nitrate loss from a restored floodplain in the Lower Cosumnes River, California. Hydrobiologia. 571(1):261–272. https://doi.org/10.1007/s10750-006-0249-2

Stoffel M, Nakagawa S, Schielzeth H. 2023. partR2 package. https://cran.r-project.org/web/packages/partR2/vignettes/Using_partR2.html

Swanson W, De Jager NR, Strauss E, Thomsen M. 2017. Effects of flood inundation and invasion by Phalaris arundinacea on nitrogen cycling in an Upper Mississippi River floodplain forest. Ecohydrology. 10(7). https://doi.org/10.1002/eco.1877

Tarboton D. 2015. David Tarboton: Hydrology research group-terrain analysis using digital elevation models (TauDEM) Version 5. Utah State University Hydrology Research Group. https://hydrology.usu.edu/taudem/taudem5/

Theiling CH, Nestler JM. 2010. River stage response to alteration of Upper Mississippi River channels, floodplains, and watersheds. Hydrobiologia. 640(1):17–47. https://doi.org/10.1007/s10750-009-0066-5

Tian H, Xu R, Pan S, Yao Y, Bian Z, Cai W-J, et al. 2020. Long-term trajectory of nitrogen loading and delivery from Mississippi River Basin to the Gulf of Mexico. Global Biogeochemical Cycles. 34(5):e2019GB006475. https://doi.org/10.1029/2019GB006475

Tiedje J, Simkins S, Groffman PM. 1989. Perspectives on measurement of denitrification in the field including recommended protocols for acetylene based methods. Plant and Soil. 115(2):261–284. https://doi.org/10.1007/BF02202594

Tockner K, Pennetzdorfer D, Reiner N, Schiemer F, Ward JV. 1999. Hydrological connectivity, and the exchange of organic matter and nutrients in a dynamic river–floodplain system (Danube, Austria). Freshwater Biol. 41(3):521–535. https://doi.org/10.1046/j.1365-2427.1999.00399.x

Tockner K, Stanford JA. 2002. Riverine floodplains: present state and future trends. Environ Conserv. 29(3):308-330. https://doi.org/10.1017/S037689290200022X

[USACE] U.S. Army Corps of Engineers. 2010. Regional supplement to the Corps of Engineers wetland delineation manual: Midwest region (version 2.0). Wetlands Regulatory Assistance Program. Report No.: ERDC/EL TR-12-9. https://www.usace.army.mil/Missions/Civil-Works/Regulatory-Program-and-Permits/reg_supp/

[USACE] U.S. Army Corps of Engineers. 2011. Wabash River Watershed: Section 729 Initial Watershed Assessment. Louisville.

Welti N, Bondar-Kunze E, Mair M, Bonin P, Wanek W, Pinay G, et al. 2012. Mimicking floodplain reconnection and disconnection using 15N mesocosm incubations. Biogeosciences. 9:4263-4278. https://doi.org/10.5194/bg-9-4263-2012

Whited DC, Lorang MS, Harner MJ, Hauer FR, Kimball JS, Stanford JA. 2007. Climate, hydrologic disturbance, and succession: Drivers of floodplain pattern. Ecology (Durham). 88(4):940–953. https://doi.org/10.1890/05-1149

Wolf KL, Ahn C, Noe GB. 2011. Microtopography enhances nitrogen cycling and removal in created mitigation wetlands. Ecol Eng. 37(9):1398–1406. https://doi.org/10.1016/j.ecoleng.2011.03.013

Wolheim WM, Harms TK, Peterson BJ, Morkeski K, Hopkinson CS, Stewart RJ, et al . 2014. Nitrate uptake dynamics of surface transient storage in stream channels and fluvial wetlands. Biogeochemistry. 120:239-257. https://doi.org/10.1007/s10533-014-9993-y

Zhou R, Yang C, Li E, Cai X, Jiao Y, Xia Y. 2021. Object-based wetland vegetation classification using multi-feature selection of unoccupied aerial vehicle RGB imagery. Remote Sens. 13(23):4910. https://doi.org/10.3390/rs13234910